Developmental Biology 365 (2012) 424–433

Contents lists available at SciVerse ScienceDirect

Developmental Biology

journal homepage: www.elsevier.com/developmentalbiology

Laser ablation of the sonic hedgehog-a-expressing cells during fin regeneration affects ray branching morphogenesis

Jing Zhang [a], Shirine Jeradi [a,1], Uwe Strähle [b], Marie-Andrée Akimenko [a,*]

[a] CAREG, Department of Biology, University of Ottawa, 30, Marie Curie, ON, Canada K1N 6N5
[b] Institute of Toxicology and Genetics, Karlsruhe Institute of Technology, Postfach 3640, 76021 Karlsruhe, Germany

ARTICLE INFO

Article history:
Received for publication 7 August 2011
Revised 21 February 2012
Accepted 8 March 2012
Available online 14 March 2012

Keywords:
Zebrafish
Fin regeneration
Ray branching
shha
Laser ablation
GFP
Transgenic line

ABSTRACT

The zebrafish fin is an excellent system to study the mechanisms of dermal bone patterning. Fin rays are segmented structures that form successive bifurcations both during ontogenesis and regeneration. Previous studies showed that *sonic hedgehog* (*shha*) may regulate regenerative bone patterning based on its expression pattern and functional analysis. The present study investigates the role of the *shha*-expressing cells in the patterning of fin ray branches. The *shha* expression domain in the basal epidermis of each fin ray splits into two prior to ray bifurcation. In addition, the osteoblast proliferation profile follows the dynamic expression pattern of *shha*. A zebrafish transgenic line, *2.4shh:gfp*ABC#15, in which GFP expression recapitulates the endogenous expression of *shha*, was used to specifically ablate *shha*-expressing cells with a laser beam. Such ablations lead to a delay in the sequence of events leading to ray bifurcation without affecting the overall growth of the fin ray. These results suggest that *shha*-expressing cells direct localized osteoblast proliferation and thus regulate branching morphogenesis. This study reveals the fin ray as a new accessible system to investigate epithelial–mesenchymal interactions leading to organ branching.

Introduction

Zebrafish are among the few vertebrates that are able to regenerate several organs, including all fins, following amputation or injury at adult stage. The caudal fin has been used as a model to study regeneration because it represents an interesting system to study bone regeneration, it is easily accessible and its amputation does not impair the life of the animal. In addition, the caudal fin of zebrafish also presents an almost symmetrical shape which allows using one of the two lobes as an internal control, reducing the effects of inter-individual variations. The major exoskeleton components of the adult fins are the rays, also named lepidotrichia, made of dermal bone. Each lepidotrichium is composed of two series of concave segments facing each other and forming the hemirays. Each ray can form successive bifurcations as the fin grows, increasing the fin surface. The two lateral rays never form branches (Quint et al., 2002). Fin amputation at the level of the dermal bony rays is followed by a quick regeneration of these rays (about 3 weeks at 28 °C). Three main steps take place during fin regeneration: 1) wound healing, during which a thin epidermal layer is established to cover the stump; then 2) formation of a blastema, which is a cluster of undifferentiated cells, between the stump and the wound epidermis; and finally, the 3) regenerate outgrowth occurs, during which the lost tissues are re-established from the differentiation zone located at the proximal end of each blastema (Akimenko et al., 2003; Poss et al., 2003). Recent studies have shown that the blastema is formed through the dedifferentiation of mature cells and as the fin regenerates, the fate of the blastema cells remains restricted to their original and respective lineages (Knopf et al., 2011; Tu and Johnson, 2011). Notably, dedifferentiated scleroblasts, the osteoblast-like cells, expressing markers of bone progenitors proliferate and re-differentiate into scleroblasts during the regenerate outgrowth step (Knopf et al., 2011; Tu and Johnson, 2011). The newly differentiated scleroblasts are lining the epidermis and release the bone matrix in the sub-epidermal space. The regenerating ray branches again during this last phase.

SHH, a member of the Hh family, is an important morphogen involved in many developmental processes of vertebrates and invertebrate species through coordination of cell proliferation, cell fate determination and patterning (Fu et al., 2004; Hutchin et al., 2005; Krause et al., 2010; Miller et al., 2004; Park et al., 2010; Yuasa et al., 2002). The secreted protein activates downstream gene expression via a signaling cascade that initiates through the binding and inactivation of the receptor Patched 1 (PTC1), a 12-pass transmembrane protein (Briscoe et al., 2001; Mullor and Guerrero, 2000). SHH is also necessary for branching morphogenesis of organs such as the lungs (Affolter et al., 2009; Gjorevski and Nelson, 2010; Miller et al.,

* Corresponding author at: Department of Biology, University of Ottawa, 30, Marie Curie, Ottawa, ON, Canada K1N 6N5. Fax: +1 613 562 5486.
E-mail addresses: jingzhang1982@gmail.com (J. Zhang), shirine.j@hotmail.com (S. Jeradi), Uwe.Straehle@itg.fzk.de (U. Strähle), makimen@uottawa.ca (M.-A. Akimenko).
[1] Present address: Institute for Developmental Biology, University of Cologne, D-50923 Cologne, Germany.

0012-1606/$ – see front matter © 2012 Elsevier Inc. All rights reserved.
doi:10.1016/j.ydbio.2012.03.008

2004), the salivary gland (Harunaga et al., 2011; Jaskoll et al., 2004) and, although results are conflicting, SHH is involved in the regulation of prostate branching (Freestone et al., 2003; Pu et al., 2004; Thomson and Marker, 2006). Branching formation depends on interactions between epithelial and mesenchymal cells (Affolter et al., 2009; Gjorevski and Nelson, 2010; Gray et al., 2010; Harunaga et al., 2011). In the lung, SHH is expressed in epithelial cells where it has been shown to be essential for branching morphogenesis. Moreover, *Shh* null mice fail to undergo normal lung branching patterns (Pepicelli et al., 1998). *Ptc1*, is expressed in the overlying mesenchyme, with a higher level of expression at the distal tip of the branch (Pepicelli et al., 1998). In the bud epithelia of the salivary gland, SHH is detected at the terminal bud, along with its receptor PTC1 (Jaskoll et al., 2004). While treating salivary gland explants with exogenous SHH peptides enhances branch formation, abrogation of the HH signaling by cyclopamine treatment leads to a decrease in branching morphogenesis (Jaskoll et al., 2004).

During zebrafish fin regeneration, *shha* is expressed in a subset of basal epithelial cells at the level of the differentiation zone, adjacent to the newly differentiating scleroblasts (Laforest et al., 1998; Quint et al., 2002). It has recently been shown that *shha* expression at this position along the proximal–distal axis of the fin regenerate is maintained through the activity of Fgf and Wnt pathways (Lee et al., 2009). *ptc1* is expressed in the basal epithelial cells in a domain that includes that of *shha* and in the adjacent newly differentiated scleroblasts (Laforest et al., 1998). Before a bifurcation occurs in each fin ray, the expression domain of *shha* separates into two except for the two lateral rays that never bifurcate (Laforest et al., 1998). This expression pattern of *shha* suggests a role for *shha*-expressing cells in branching morphogenesis of the regenerating rays. Supporting this hypothesis, amputation of the caudal fin immediately after a branching point will result in sister ray fusion that correlates with a single set of *shha*-expressing cells in the ray, suggesting that a correct distribution of the *shha*-expressing cells may be required for branch formation (Laforest et al., 1998). Consistently, ectopic expression of *shha* in the tissue between sister ray branches leads to ectopic bone deposition and therefore fusion of the branches (Quint et al., 2002). Finally, inhibition of hedgehog signaling by cyclopamine treatments not only affected blastema cell proliferation but also scleroblast patterning (Lee et al., 2009; Quint et al., 2002). Thus, in the fin regenerate, *shha* signaling seems to be involved in patterning the lepidotrichia.

In this report, we dissect the specific role of *shha*-expressing cells during zebrafish caudal fin regeneration by ablating them using a laser beam. The technique of laser cell ablation has been shown to be efficient in determining the function of specific cell types in zebrafish embryos and larvae (Abraham et al., 2010; Greenspoon et al., 1995; Li et al., 2003; Roeser and Baier, 2003; Wu et al., 2011). We used the *2.4shh:gfp*:ABC#15 zebrafish transgenic line (Ertzer et al., 2007) in which GFP expression recapitulates the endogenous expression of *shha*. Our results suggest that *shha*-expressing cells may play a role in patterning the ray fin branches through interactions with adjacent scleroblasts.

Materials and methods

Animal maintenance

Fish used in all experiments are maintained at 28.5 °C with a photo period of 14 h of light and 10 h of darkness, and fed regularly (Westerfield, 1993).

Fin amputation

Adult zebrafish of at least 10 weeks of age were anesthetized by immersion in water containing 0.6 M tricaine (ethyl-aminobenzoate; Westerfield, 1993). Caudal fins of adult fish were amputated, using a scalpel blade, 1–2 segments proximal to the first branch point of the lepidotrichia. Fish were then returned to fresh system water to recover.

Fluorescence imaging

Zebrafish were anesthetized as described above and placed on the surface of a 1.5% agarose plate. The caudal fins spread naturally. Imaging was performed using a dissection microscope (Leica MZ FLIII) or a Zeiss Axioskop compound microscope equipped with a digital camera (Zeiss AxioCam HRm) and AxioVision AC software.

Laser cell ablation

Zebrafish at 3 dpa were anesthetized as described above and placed in a small chamber ($L \times W \times H = 4 \times 2 \times 0.5$ cm) filled with anesthetic solution. The caudal fin was flattened and held down with a slice hold-down (Warner Instruments, Cat#64-0248). A VSL-337ND-S laser system (Spectra-Physics) was installed on a Zeiss Axioskop compound microscope. Cell ablation was performed with a laser beam of 435 nm aimed at the GFP cells in the fin regenerate via a 40× water immersion objective and by applying 30 Hz laser pulses for about 5 s on each cell. Small air bubbles were occasionally observed immediately after giving laser pulses; the presence of such bubbles has been described as a sign of optimal laser power (Roeser and Baier, 2003). These bubbles persisted for a few seconds (maximum 1 or 2 min) and disappeared. Since the bubbles persist for a very short time, they most likely do not impact on fin recovery.

Lipophilic carbocyanine dye (Di-I) labeling

A 0.25% w/v stock solution of Di-I (1,19-dioctadecyl-3,3,39,39-tetramethyl indocarbocyanine perchlorate; Molecular Probes, Eugene, OR) in ethanol was further diluted tenfold in a 45 °C 0.3 M sucrose solution prior to microinjection. Di-I was injected into the blastema of the fin regenerates at 3 dpa with a Narishige IM300 Microinjector (Poleo et al., 2001). An injection of 30 ms and 20 psi delivered a small bolus of dye solution in the desired region, whereupon a small pink dot was visible. The lipophilic carbocyanine dye inserts into the membrane of the cells adjacent to the injection site. After 24 h, when single or small clusters of cells labeled with Di-I were distinguishable, some of these clusters of cells were processed for laser ablation.

In situ hybridization

In situ hybridization on whole mount and cryostat sections of fin regenerates were performed as previously described (Smith et al., 2008). For *in situ* hybridization on sections shown in Fig. 5, consecutive sections of fin regenerates were collected on 3 slides. For each regenerate, the first slide was mounted to observe GFP fluorescence, the second and third slides were processed for *in situ* hybridization with *dlx5a* and *col10a1*, respectively. After imaging, the slides of *in situ* hybridization with *col10a1* were processed again for Sirius red staining. Anti-sense RNA probes were synthesized as previously described: *shha* (Smith et al., 2006), *dlx5a* (Akimenko et al., 1994), and *col10a1* (Avaron et al., 2006). A 0.7 kb fragment of the GFP cDNA was obtained by PCR from the *shh:gfp*:ABC construct using forward primer 5′-ATGAGTAAAGGAGAAGAACTTTTCA-3′ and reverse primer 5′-TTTGTATAGTTCATCCATGCCA-3′. The PCR product was then inserted into pDrive. To make an anti-sense RNA probe, the plasmid DNA was linearized with *Xho*I and transcribed *in vitro* with T7 RNA polymerase. *In situ* hybridization on cryostat sections were mounted with coverslips and Aqua Poly/Mount (Polysciences, Cat#18606) before imaging.

Picrosirius red staining

Picrosirius red staining on cryostat sections was performed as previously described (Smith et al., 2008). For picrosirius red staining shown in Fig. 5, we used the sections that had been first processed for *in situ* hybridization with *col10a1* probe. After imaging for *col10a1* expression, the coverslips and mounting medium were removed by overnight immersion of the slides in water and the section were stained with picrosirius red.

Immunodetection of cell proliferation

Fin regenerates were fixed with 9:1 formaldehyde (37%):ethanol (95%) overnight at 4 °C (Vihtelic and Hyde, 2000) and cryosectioned for detection of cell proliferation using the proliferating cell nuclear antigen (PCNA) immunostaining. A mouse anti-PCNA antibody (Clone PC10, Dako, Cat#M0879) was used at 1:250 dilution and a fluorescently labeled secondary anti-mouse antibody (Alexa Fluor® 488 Goat Anti-mouse IgG (H+L), Invitrogen Cat#A11001) used at a 1:500 dilution. The slides were then mounted with VECTASHIELD® Mounting Medium with DAPI (Vector Laboratories, Inc. cat#H-1200) before imaging.

Results

Time course analysis of shha domain of expression during branching morphogenesis of the lepidotrichia in the fin regenerate using the 2.4shh:gfp:ABC#15 transgenic line

GFP expression in the *2.4shh:gfp*:ABC#15 transgenic line recapitulates the endogenous expression of *shha*. During regeneration of *2.4shh:gfp*:ABC#15 zebrafish fins, groups of GFP+ cells are located in the distal region of lepidotrichia (Fig. 1A). At 2 days post amputation (dpa), a few GFP+ cells start to be visible in the area where the blastema is newly formed (Fig. 1B). At 2.5 dpa, the areas of GFP expression are elongated and a single group of the GFP+ cells is clearly visible in each fin ray (Fig. 1C). By 3 dpa, the GFP-expressing domain starts to show signs of splitting at the proximal end (Fig. 1D). At 4 dpa, a clear separation along the proximal–distal axis is observed at the midline through the whole GFP-expressing domains (Fig. 1E). At 5 dpa, the separation becomes more prominent and the weak fluorescence in the cleavage is not visible anymore (Fig. 1F). Meanwhile, although the separation was initiated at the proximal end of the GFP expression domain, distal GFP expression domains are now clearly separated, reflecting the branching process. Longitudinal section of a 4 dpa fin regenerate shows that the GFP+ cells are located in the basal cell layer of the epidermis (Fig. 1G), and correlates with the endogenous domain of expression of *shha* as shown by *in situ* hybridization (Fig. 1H). The GFP expression domains in the fin regenerate are slightly larger than the *shha*-expressing domains previously observed by *in situ* hybridization (Laforest et al., 1998). One possible explanation could be the presence of GFP protein that persists in cells after the transcription of *shha* has diminished. When *in situ* hybridization of *shha* and *gfp* anti sense RNA probes was carried in each lobe of a 6 dpa fin regenerate, similar expression patterns are seen for *shha* and *gfp* transcripts (Figs. 1I–L).

Altogether, these results show that the expression pattern of GFP in the *2.4shh:gfp*:ABC#15 transgenic line recapitulates that of endogenous *shha*.

Localized proliferation of basal epidermal cells and scleroblasts on both sides of the hemiray during branching morphogenesis

As SHH signaling has been shown to have a mitogenic role in lung and salivary gland branching morphogenesis (Bellusci et al., 1997a; Jaskoll et al., 2004), we examined whether cell proliferation may

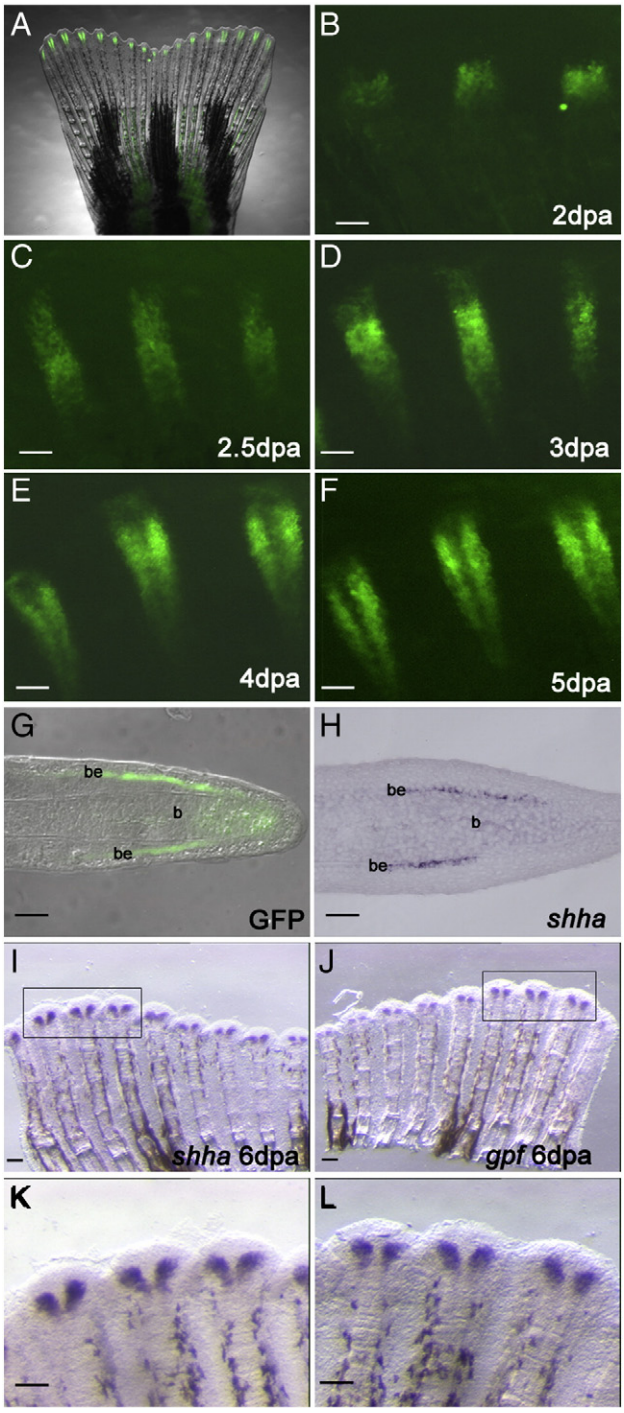

Fig. 1. GFP expression recapitulates the endogenous *shha* expression in the zebrafish transgenic line *2.4shha:gfp*ABC#15. (A) Bright field and fluorescent images of the caudal fin merge show GFP expression in an intact fin of a *2.4shha:gfp*ABC#15 transgenic fish. (B–F) Higher magnification of whole-mount images of a few fin rays at different stages of regeneration. (B) At 2 days post amputation (dpa), GFP is expressed in a few cells at the level of the blastema. (C) At 2.5 dpa, GFP expression is restricted to one single domain. (D) At 3 dpa, cleavages start to appear at the proximal end of the GFP-expressing domain and in some rays these cleavages are extending distally. (E) At 4 dpa, a clear separation is visible, and in (F) it is more prominent at 5 dpa. (G) Longitudinal section of a fin regenerate of a *2.4shha:gfp*ABC#15 transgenic fish at 4 dpa shows GFP expression in the basal layer of the epidermis. (H) *In situ* hybridization on a longitudinal section of a 4 dpa fin regenerate shows endogenous *shha* expression in the basal layer of the epidermis. (I–L) *In situ* hybridization performed on the two lobes of the same fin regenerate at 6 dpa show that *shha* (I and K) and *gfp* (J and L) are expressed in the same cell population. The areas indicated by black boxes in I and J are enlarged in K and L. Scale bars in G and H: 20 μm; all other panels: 100 μm. be: basal layer of epidermis; b: blastema.

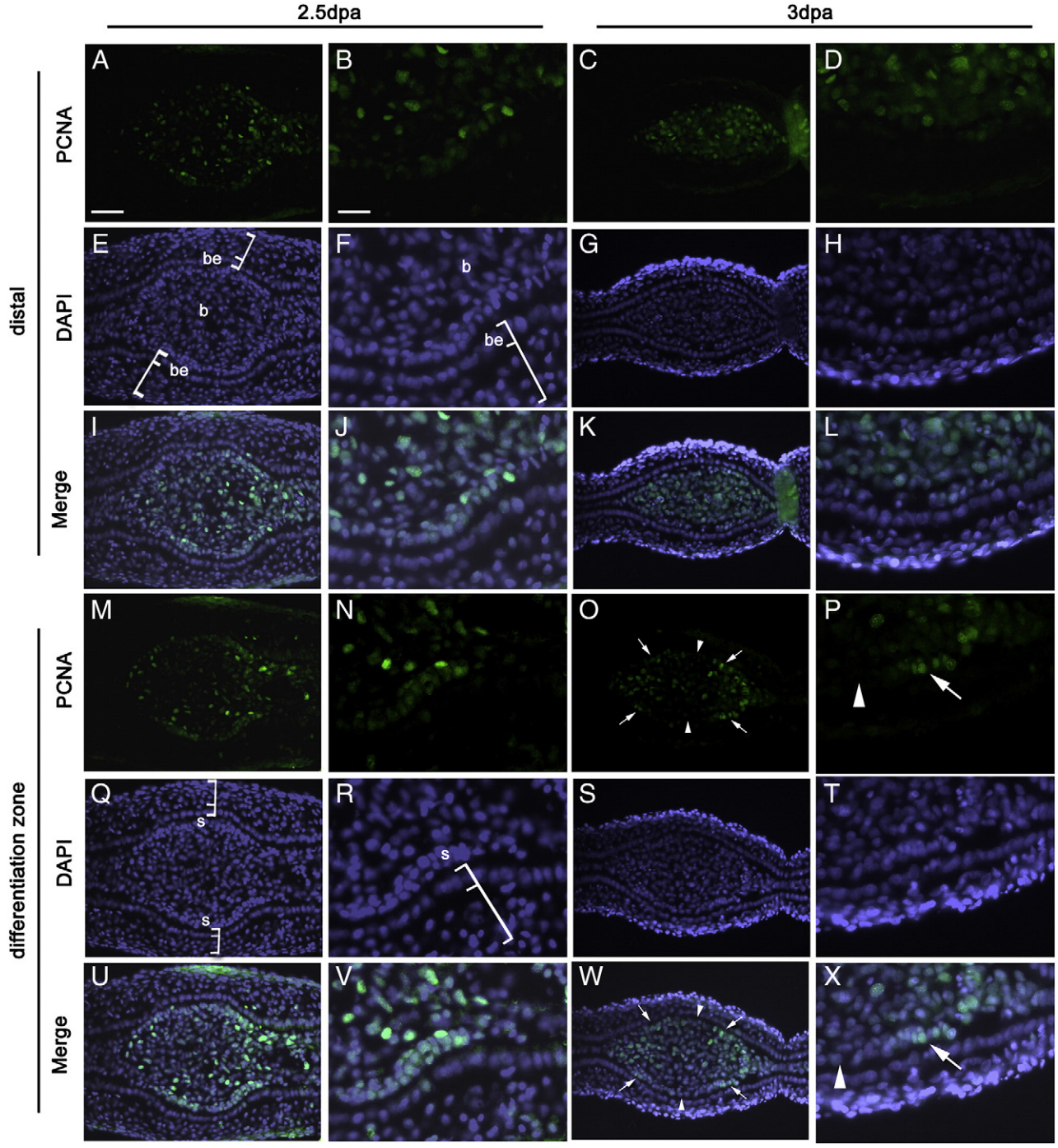

Fig. 2. Localized cell proliferation accompanies branch formation. Cell proliferation was detected by immunofluorescence (green) using the proliferating cell nuclear antigen (PCNA) antibody on transverse sections of fin regenerates at 2.5 dpa (A, B, M and N) and 3 dpa (C, D, O and P). DAPI staining (blue) of the same sections is shown in E–H and Q–T. The merged images of the corresponding PCNA and DAPI staining are shown in I–L and U–X. B, F, J, N, R, V, D, H, L, P, T, and X are enlargement of small areas of A, E, I, M, Q, U, C, G, K, O, S, and W, respectively. (A and B) In sections corresponding to the distal part of the fin regenerate at 2.5 dpa, PCNA positive cells are abundant in the blastema. There is no PCNA+ cells in the epidermis. (C and D) At 3 dpa, the distribution of PCNA+ cells in the distal regenerate is similar to that in (A). (M and N) At 2.5 dpa, in sections corresponding to the differentiation zone, PCNA+ cells are more concentrated in the scleroblasts lining the epidermis than in the center of the connective tissue. (O and P) At 3 dpa, as at 2.5 dpa (M), there is a higher concentration of PCNA+ cells in scleroblasts than in the central part of the ray but in contrast to 2.5 dpa, the proliferating scleroblasts are localized on the two lateral sides of the hemiray. Note: Bright PCNA staining corresponds to cells that are actively proliferating at the time of tissue fixation. Some residual staining in cells of the connective tissue reflects the past proliferative state of these cells. Arrows in (O, P, W and X) indicate the localized proliferation of the scleroblasts. Arrowheads in (O, P, W and X) indicate the central scleroblasts that show no PCNA signal. Brackets in E, F, Q and R indicate the epidermis. Scale bars: A, E, I, M, Q, U, C, G, K, O, S and W (shown in A) = 20 μm; B, F, J, N, R, V, D, H, L, P, T and X (shown in B) = 7 μm. be: basal layer of epidermis; b: blastema; s: scleroblast.

account for the formation of new ray branches using PCNA (Proliferating Cell Nuclear Antigen) immunostaining on transverse sections of fin regenerates. PCNA immunostaining, as well as DAPI staining to show the nuclei are shown in Fig. 2. At 2.5 and 3 dpa, the distal part of the regenerate is made of a large population of blastema cells that show a strong PCNA staining as expected. In contrast, there is little if any proliferation in the epidermis (Figs. 2A, B, C and D). In the differentiation zone, at a level corresponding to the *shha* expression domain, there is a decrease in cell proliferation in the center of the connective tissue but proliferation persists in the scleroblasts

(Figs. 2M, N, O and P). However, the distribution of proliferating scleroblasts differs between 2.5 and 3 dpa. At 2.5 dpa, PCNA staining is observed in most of the scleroblasts lining the epidermis in all rays examined (n = 7) (Figs. 2M and N). At 3 dpa, when domains of GFP+ and *shha*-expressing cells are separating into two regions, PCNA staining is restricted to the lateral scleroblasts of each hemiray in 52% of the rays examined (n = 23) (Figs. 2O and P).

Shha-expressing cells can specifically be ablated using a laser beam

To further investigate the role of *shha*-expressing cells in branching morphogenesis during fin regeneration, a laser-mediated approach was used to ablate these cells *in vivo* using the *2.4shh:gfp*ABC#15 transgenic line. The *shha*-expressing cells are located in one-cell layer and the epithelium above these cells is optically clear, which makes laser ablation feasible.

To verify that the laser-ablation technique can efficiently and specifically eliminate *shha*-expressing cells, several control experiments were performed. First, we verified that laser cell ablation does not induce any sign of damage to the fin regenerate surrounding the targeted area (Figs. 3A–D).

The efficiency of laser cell ablation was further verified by ablating epithelial cells labeled with DiI, a fluorescent vital dye. The DiI solution was microinjected into the epithelial layers of fin regenerates at 3 dpa. One day later, when laser cell ablation was performed on single cell or small clusters of DiI-labeled cells, fluorescence of the targeted cells disappeared within 5 s (Figs. 3E and F). To verify that under these conditions the laser beam actually causes cell ablation but not simply photobleaching of the GFP fluorescence, we targeted cell types easily distinguishable from other cell types by their specific pigmentation. For example, immobile blood cells that are trapped in the newly formed plexus in the regenerate were successfully ablated (data not shown) even though they are located deeper into the tissue than *shha:gfp*-expressing cells.

Finally, immediately after ablation of *shha*-expressing cells at 3 dpa, *shha* expression was barely detectable in the fin rays in which cells were ablated compared to the adjacent fin rays used as controls (Figs. 3G and H). We also examined, immediately after laser ablation, transcripts of *col10a1* which are expressed in both the basal layer of the epidermis, in a domain partially overlapping that of *shha*-expressing cells, as well as in the adjacent scleroblasts (Fig. 3I). Expression of *col10a1* in the basal layer of the epidermis is diminished in the area where the laser beam was focused, while the adjacent scleroblasts showed no visible changes in expression (Fig. 3J).

Altogether, these results show that the technique of laser cell ablation is efficient and results in the specific loss of *shha*-expressing cells in fin regenerates.

Laser ablation of shha-expressing cells induces a delay in ray branching

Before examining the effects of cell ablation on ray branching, the variations in branching morphogenesis under normal regeneration conditions were determined. We compared the position of the origin of the first bifurcation of five ventral and of five corresponding dorsal fin rays in the same regenerate at 21 dpa (Fig. 4A). A variation of less than 1 segment between ventral and dorsal fin rays was observed in 63.3% of the rays (n = 30). In 36.63% of the rays, the variations were more than 1 segment but less than 2 segments. Finally, this variation was more than 2 segments in only 0.07% of the rays examined (Fig. 4B). We then examined the effects of ablating the shha-expressing cells on branching morphogenesis at a time at which there is still one domain of GFP expression per ray. Ablation was performed in five consecutive rays of one lobe and these were later compared to the corresponding rays of the other lobe. At 20 days post laser ablation (dpl), 42% (n = 55) of the rays where ablation had been performed showed a branching delay of more than two segments compared to internal controls (Figs. 4C and D).

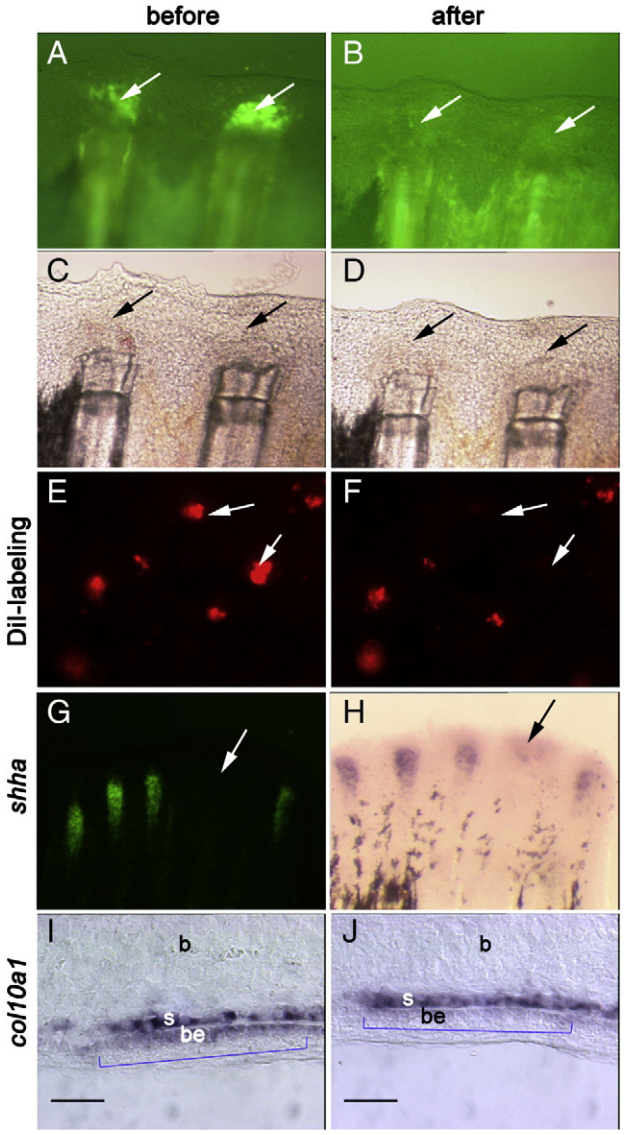

Fig. 3. Controls for the method of laser cell ablation on fin regenerate. Pictures of fin rays were taken before (A, C and E) and immediately after (B, D and F) laser ablation of different cell types of the fin. (A) *Shha:gfp*-expressing cells in two rays of the *2.4shha:gfp*ABC#15 transgenic line at 2 dpa. (B) After laser ablation of the cells shown in (A), GFP fluorescence disappears. (C and D) Bright field images of the rays shown in (A and B), respectively, show no visible damage to the tissue following laser ablation. (E) A few epidermal cells of the fin regenerate were labeled by injection of DiI. (F) DiI fluorescence disappears following laser ablation of the targeted cells (arrows in E and F). (G) Fluorescent image of a fin regenerate following ablation of the GFP positive cells in one ray. (H) *In situ* hybridization immediately after laser ablation of the fin shown in (G) shows *shha* expression in each fin ray except in the ray on which ablation has been performed. (I and J) *In situ* hybridization on longitudinal sections of a fin ray with *col10a1* probe. (I) Before ablation, *col10a1* is expressed in the basal layer of the epidermis (where *shha:gfp* is also expressed) and in the adjacent scleroblasts. (J) Following ablation of the GFP positive epidermal cells, *col10a1* expression in the basal epidermal cells disappears, while *col10a1* expression in the scleroblasts remains unchanged. Arrows in (A–H), and the blue brackets in (I and J) indicate the cells targeted for laser ablation. Scale bar in panels I, J = 20 μm.

We also examined whether laser ablation affected the growth of the regenerate. To this end, the length of the ventral (Lv) and dorsal (Ld) ray regenerate corresponding to the distance between the amputation level and the tip of a given ray was measured at 23 dpa. The percentage difference in length between the corresponding dorsal and ventral rays (n = 55) was calculated with the equation (Lv − Ld)/Ld. At 23 dpa, the average percentage difference in length

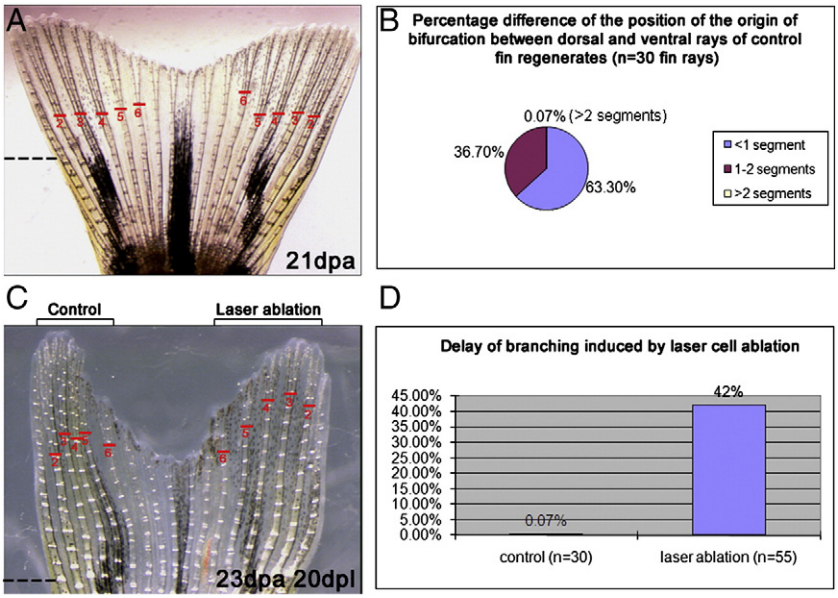

Fig. 4. Laser ablation induces a delay of ray branching. (A) Caudal fin regenerate observed at 21 days following amputation below the first branching point of the rays. Ray numbers are shown in red; the corresponding rays on the ventral and dorsal lobes have the same number (ray 1 that never forms bifurcation is not indicated). Red lines indicate the position of the first branching point of five ray regenerates of the ventral and dorsal lobes, respectively. (B) percentage difference in the position of the origin of bifurcation (measured in number of segments) between the corresponding rays of the dorsal and ventral lobes observed in fin regenerates (n = 30) at 21 dpa. Only 0.07% of the rays show a difference greater than 2 segments of the origin of bifurcation. (C) Fin regenerate at 20 dpl of a *2.4shh:gfp*ABC#15 transgenic fish after laser cell ablation of the GFP positive cells in rays 2, 3, 4, of the ventral lobe at 3 dpa. The red lines indicate the origin of bifurcation in rays 2, 3, 4 in the control side and the side where laser ablation has been performed, respectively. (D) Graph showing the percentage of rays presenting a difference greater than 2 segments in the position of the origin of bifurcation between the ventral and dorsal lobes, in control fins (no ablation) (left bar) and in experimental fins (right bar) in which GFP positive cells have been ablated in rays of the ventral lobe. Dashed lines indicate the level of amputation.

between dorsal and ventral fin rays of control fin rays (normal regenerate without cell ablation) was 1.28% and 3.10% (P = 0.333) between dorsal (control) and ventral (containing fin rays subjected to laser ablation) fin rays. This result indicates that there is no significant growth delay in the regenerate.

Altogether, these results suggest that laser ablation of the *shha*-expressing cells induced a significant delay in ray branching during fin regeneration, while it did not have any effects on overall regenerative growth.

The division of the shha domain of expression precedes the subdivision of the domain of expression of dlx5a, col10a1 and of the bone matrix

Since ablation of the *shha* expressing epithelial cells leads to defects in bone patterning, we compared the expression of genes related to bone formation with GFP expression and branching morphogenesis. To better demonstrate the positional features of gene expression and the morphology of the lepidotrichia, GFP analysis, *in situ* hybridization for *dlx5a* and *col10a1*, and picrosirius red staining were performed on consecutive transverse sections of fin regenerates. At all stages investigated (2, 2.5, 3, 3.5, 4, and 5dpa), *dlx5a* is expressed in the scleroblasts of the differentiation zone (Figs. 5B, F, J and N) and *col10a1* is expressed in both the basal cell layer of the epidermis and the scleroblasts (Figs. 5C, G, K and O). Four different patterns of expression were observed when GFP, *dlx5a* and *col10a1* expression were compared. Pattern I: the expression of GFP, *dlx5a* and *col10a1* were all in a single domain (Figs. 5A–D); pattern II: the expression domain of GFP was separated into two while *dlx5a* and *col10a1* expression was still within a single domain (Figs. 5E–H); pattern III: the expression domain of GFP and *dlx5a* were separated into two but *col10a1* was still expressed in a single domain (Figs. 5I–L); pattern IV: the expression domains of GFP, *dlx5a* and *col10a1* were all separated into two (Figs. 5M–P). The percentage of each pattern observed at various time points are shown in Fig. 5Q. At 2 dpa, all rays only showed pattern I. Between 2 and 5 dpa, the expression domains of GFP, *dlx5a* and *col10a1* were undergoing a separation, and this process was completed by 5 dpa. In the rays examined, the expression domain of *col10a1* never split before that of GFP or of *dlx5a*. Moreover, the expression domain of *dlx5*a never split before that of GFP. Sirius red staining of the collagenous tissue, only revealed the basement membrane between the basal epithelial layer and the scleroblasts (Figs. 5D, H, L and P). This observation suggests that, at this position along the distal–proximal axis, there is no or very little bone matrix deposition indicating that splitting of the GFP, *dlx5a*, and *col10a1* expression domains precedes bone formation. Altogether, these observations indicate that the expression domains of *shha*, *dlx5a* and *col10a1* split in a sequential manner, with *shha* splitting first, then *dlx5a* and finally *col10a1*, and all of these precede branching of the lepidotrichia.

Ablation of shha-expressing cells delays the division of the domain of expression of scleroblast markers

We then examined the effects of ablating *shha*-expressing cells on the expression patterns of *dlx5a* and *col10a1*. Laser cell ablation was performed at 3 dpa on one ventral ray and the corresponding dorsal ray was used as a control. At 6 dpa (3dpl), fin regenerates were photographed (Figs. 6A and E) and sectioned for *in situ* hybridization with *dlx5a* (Figs. 6B and F) or *col10a1* (Figs. 6C and G) probes, or stained with Sirius red (Figs. 6D and H). At 6 dpa (3 dpl), GFP was expressed in a normal pattern in the control fin rays (Fig. 6A). In the fin rays subjected to laser ablation, however, the GFP expression domain just started to show the separation at the center (9/15 rays, Fig. 6E), which is the pattern normally seen at around 4 dpa. The expression of *dlx5a* in the laser-ablated fin rays remained as one domain (2/4 rays, Fig. 6F) whereas it had already split into two in control rays (Fig. 6B). This difference was also observed for *col10a1* (3/4 rays, Figs. 6C and G). Sirius red staining also confirmed the presence of a bifurcation in control rays (Fig. 6D) but not in rays subjected to laser ablation (Fig. 6H) despite the fact that both control and laser-ablated rays had regenerated to a similar distance from the plane of amputation.

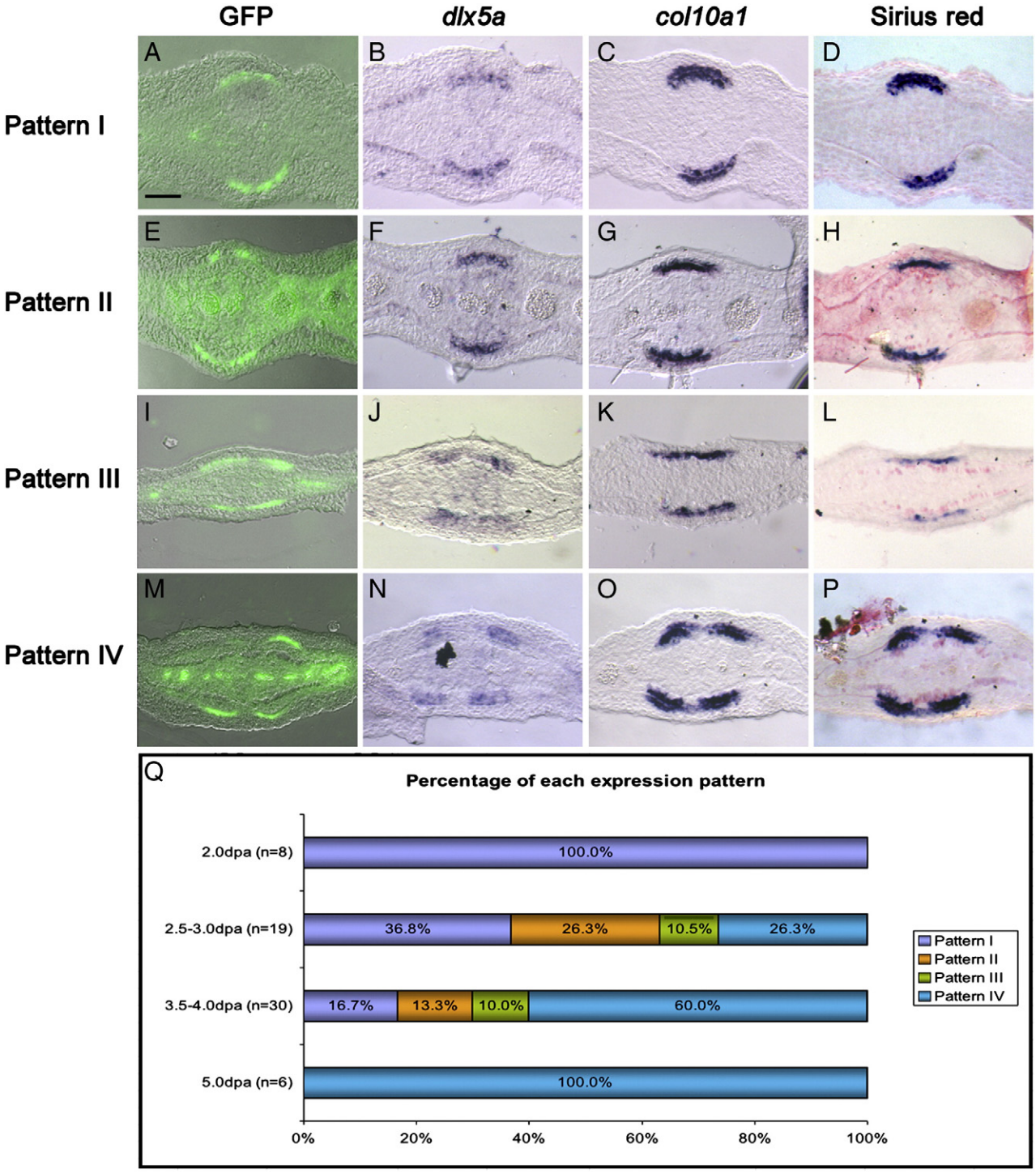

Fig. 5. Separation of GFP domain of expression into two precedes separation of the domains of expression of bone markers and bone matrix. Representative examples of the four patterns of expression of GFP (A, E, I and M), *dlx5a* (B, F, J and N), *col10a1* (C, G, K and O) observed in consecutive transverse sections of fin rays collected between 2 and 5 dpa. (D, H, L and P) Picrosirius red staining of the sections shown in (C, G, K and O), respectively. (Q) Percentages of fin rays showing pattern I (A–D), pattern II (E–H), pattern III (I–L), and pattern IV (M–P) at 2.0 dpa, 2.5–3.0 dpa, 3.5–4.0 dpa and 5 pda. Scale bar (all panels): 20 μm.

Discussion

In this report, a laser-mediated procedure was established to ablate *shha*-expressing cells during fin regeneration. Branching delays were observed in the fin rays from which the *shha*-expressing cells were removed. This defect correlated with an altered expression pattern of *dlx5a* and *col10a1*. We also show that the segregation of the *shha*-expressing cells into two domains during branching morphogenesis correlates with the distribution of proliferating scleroblasts (osteoblasts-like). This may indicate a potential role for *shha*-expressing cells in the control of scleroblast proliferation.

The method of laser ablation

In the current study, laser cell ablation was applied on adult zebrafish for the first time. This method has been previously successfully applied on zebrafish embryos and larvae to study the function of specific cell types. For example, laser ablation of GFP-expressing cells in

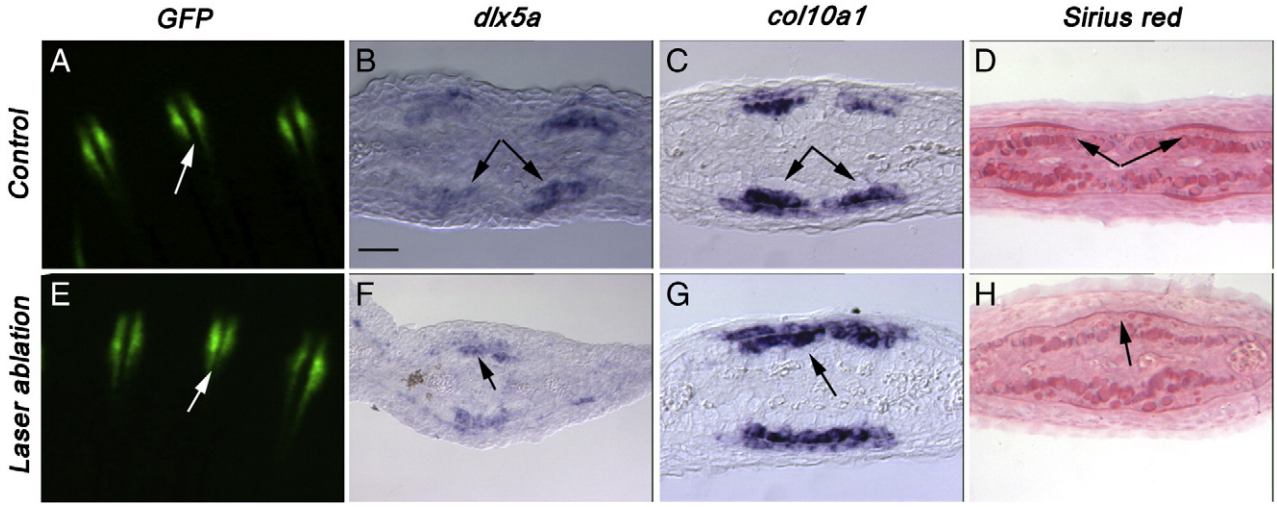

Fig. 6. Laser ablation induces a delay in the splitting of the domain of expression of *dlx5a* and *col10a1*. At 6 dpa 3 dpl, control (A, B, C and D) and laser-ablated fin rays (E, F, G and H) were observed for GFP expression (A and E) or collected for gene expression analysis (B, C, D and F) or picrosirius red staining (G and H) on transverse sections. In control fin regenerates, at 6 dpa, (A) GFP expression (B) *dlx5a*, (C) *col10a1* and (D) picrosirius red staining are observed in two separate domains. In experimental fin rays, at 6 dpa, 3 days after ablation of the GFP positive cells, (E) GFP expression is starting to separate in two domains while (F) *dlx5a*, (G) *col10a1* and (H) picrosirius red staining are still observed in a unique domain in each fin ray. Arrows indicate one or two domains of expression/staining per fin ray. Scale bar in panels B–H = 20 μm.

the optic tectum induces defects in the visuomotor behaviors of zebrafish larvae (Roeser and Baier, 2003), and laser ablation of the cardiac premigratory neural crest at the three- to four-somite stage resulted in failure of the heart tube to undergo looping (Li et al., 2003). More recently, laser ablation has also been used as a lesion-inducing method of the cilia of the hair cells in the zebrafish inner ear (Wu et al., 2011) and of gonadotropin releasing hormone (GnRH) neurons in the olfactory regions in zebrafish embryos and larvae (Abraham et al., 2010). Based on these earlier reports, we adapted this method to adult fish. Since the purpose of utilizing laser cell ablation is to kill specific cells, two major issues regarding this technique had to be addressed: 1) the efficiency (whether the targeted cells are actually killed) and 2) the specificity (whether only the targeted cells are killed). The efficiency of this method was confirmed in control experiments. Notably, *In situ* hybridization with *col10a1* on fin regenerates collected immediately after laser ablation showed that the scleroblasts were intact, indicating that the *shha:gfp*-expressing cells were ablated specifically. We cannot rule out the possibility that some scleroblasts and/or other cells adjacent or close to the *shha*-expressing cells had been ablated because of heat and free radical generation that can spread to other cells, an intrinsic problem of many lesion-inducing techniques, such as surgical, genetic manipulation, or toxin injections. However, the effect of the laser cell ablation in regenerates was mild as shown by an absence of a delay in overall growth.

Shha-expressing cells may regulate branching morphogenesis by mediating the site-directed proliferation of scleroblasts

We observed that the Shha-expressing cells are adjacent to proliferating scleroblasts before, during and after branch formation suggesting that the *shha*-expressing cells may direct the proliferation of scleroblast progenitors. When *shha*-expressing cells are present as a single domain, their induction of scleroblast proliferation would ensure the longitudinal outgrowth of the ray. As *shha*-expressing cells separate, they would instead induce lateral cell proliferation. Shha may be the signal mediating the directed proliferation of scleroblasts. SHH has been shown to possess a mitotic activity in various systems. For example, $Shh^{-/-}$ mouse or cyclopamine-treated wild-type mouse show a proliferative defect in lung mesenchymal cells (Li et al., 2004), inactivation of Hedgehog signal leads to regression of basal cell carcinoma accompanied by reduced tumor cell proliferation and increased apoptosis (Hutchin et al., 2005), and SHH signaling has been shown to control the mesenchymal proliferation for digit-patterning in chick wings (Towers et al., 2008). In addition, during zebrafish caudal fin regeneration, Hh signaling pathway is required to maintain regenerate outgrowth: inhibition of Hh signaling *via* cyclopamine leads to regenerate growth arrest and inhibition of blastema cell proliferation (Quint et al., 2002). Through induction of site-directed proliferation, Hh signaling may also regulate branching morphogenesis. When *shha*-expressing cells separate into two domains, medially located scleroblasts are deprived from Shha pro-mitotic signals and stop proliferating, while lateral scleroblasts that are still receiving Shha signals keep proliferating, leading to formation of branches.

The potential role of Shha in directing branching morphogenesis is reminiscent of the role of SHH in branching morphogenesis of the mammalian lung and salivary glands (Affolter et al., 2009; Gjorevski and Nelson, 2010; Harunaga et al., 2011). Both of these organs develop through epithelial–mesenchymal interactions that involve a cross-talk between SHH and FGF10 in the epithelium and mesenchyme, respectively (Bellusci et al., 1997b; Harunaga et al., 2011; Jaskoll et al., 2004; Pepicelli et al., 1998; Sekine et al., 1999). The modulation of the SHH/FGF feedback loop regulates the directed proliferation of cells at the origin of branching morphogenesis in these organs (Bellusci et al., 1997b; Harunaga et al., 2011; Jaskoll et al., 2004; Kim et al., 2009; Patel et al., 2006; Pepicelli et al., 1998). Accumulation of the extracellular matrix between the epithelial and the mesenchyme is also part of the mechanism leading to branching morphogenesis in both lungs, salivary gland and the fin rays (Andreasen et al., 2007; Moore et al., 2005; Patel et al., 2006). The fact that laser ablation of the *shha*-expressing cells delays fin ray branch formation argues in favor of a role for these cells in the regulation of scleroblast position in the hemiray.

Although the exact mechanisms by which *shha*-expressing cells are involved in promoting branch formation have yet to be fully elucidated, previous studies have shown that ectopic expression of *shha* induces ectopic bone deposition in the fin ray in a site-directed manner through the induction of its downstream target, *bmp2b* (Quint et al., 2002). Many studies have shown that DLX5 is activated in response to BMP2 signaling during skeletal development (Harris et al., 2003; Kim et al., 2004; Lee et al., 2003a, 2003b). DLX5 is a transcription factor expressed in developing skeleton tissues in various organisms (Akimenko et al., 1994; Ellies et al., 1997; Ferrari et al., 1995; Zhao et al., 1994). It has been shown to have an antiproliferative

effect and is acting as a positive regulator of chondrocyte and osteoblast differentiation (Chin et al., 2007; Ferrari and Kosher, 2002; Zhu and Bendall, 2009). Interestingly, a recent study revealed that ectopic expression of DLX5 (and DLX2) in avian embryos can induce, in response to local signals, aggregation of mesenchymal cells to initiate cartilage as well as intramembranous bone formation during craniofacial skeletal development (Gordon et al., 2010; Levi et al., 2006; Vieux-Rochas et al., 2010). Mesenchymal aggregates resulting from DLX induction were observed in close contact with epithelial tissue. DLX5 is known to activate RUNX2 expression, an essential transcriptional factor for osteoblast differentiation and chondrocyte maturation and a direct activator of COL10A1 expression. We previously showed that the two paralogs *runx2a* and *runx2b* are expressed in the differentiating scleroblasts of the fin regenerate (Smith et al., 2006). Here we show that, in the fin regenerate, *dlx5a* and *col10a1* (Fig. 2), as well as *bmp2b* (data not shown), are expressed in a single set of cells until *shha*-expressing cells separate into two distinct domains. This suggests a chronological succession of events for bone formation starting by a signal, e.g. Shha and/or Bmp2b, coming from the basal epithelial cells that would activate Dlx5 expression in scleroblast precursors. In turn, Dlx5 would initiate their differentiation into bone matrix producing scleroblasts. Therefore, during ray branching morphogenesis, scleroblasts separation would be dependent on the separation of *shha*-expressing cells. Indeed, we observed that separation of the *dlx5a* and *col10a1* expression domains was delayed in rays with ablated *shha:gfp*-expressing cells, correlating with the delayed separation of separation and branching morphogenesis. These observations suggest that signal(s) coming from the *shha*-expressing cells might direct scleroblasts separation. Temporary absence of these epithelial cells results in a delayed 'splitting signal', that explains the delayed scleroblast separation and bifurcation.

The shha-expressing cells may represent a signaling center for branching morphogenesis

We cannot, at this point, rule out the involvement of factors co-expressed with Shha in the branching process. One such factor could be Lymphoid Enhancer Factor 1, Lef1, a member of the Wnt/β-catenin signaling pathway (Eastman and Grosschedl, 1999). Targeted inactivation of LEF1 abrogates the formation of organs that depend on epithelial–mesenchymal tissue interactions, such as mammary glands, whiskers, teeth, and body hair during mouse embryonic development (Boras-Granic et al., 2006; Fujimori et al., 2010; van Genderen et al., 1994; Widelitz et al., 2000). Requirement for *Lef1* expression in both mesenchymal and epithelial tissue has been demonstrated (Boras-Granic et al., 2006; Fujimori et al., 2010; Kratochwil et al., 1996). During zebrafish fin regeneration, Lef1 was proposed to play a role similar to that of Shha in patterning the dermoskeletal elements (Poss et al., 2000). *lef1* is expressed in the same cells as *shha* and treatment of fin regenerates with retinoic acid or the synthetic Fgfr1 inhibitor SU5402 down-regulates *lef1* expression in the epidermis, similar to their effects on *shha* expression. Therefore, the laser-induced defects in bone patterning that we observed could also result from the disruption of Wnt signaling or from the loss of other factors. Nevertheless, the *shha*-expressing cells may constitute a signaling center which is located at the differentiation zone of the regenerative bones and may orchestrate the different signal cascades that enable the epithelial–mesenchymal interaction. It would be of great interest to characterize other genes that are also expressed in this signaling center to better understand the mechanisms of branching morphogenesis.

A possible signal threshold may regulate the timing of ray branching

As described in this report, *shha:gfp*-expressing cells first appear sparsely in the fin regenerate at 2 dpa. As regeneration proceeds, the number of *shha:gfp*-expressing cells increases and eventually reaches the point where the domain of expression separates into two. This progression may indicate that a threshold in the number of the *shha*-expressing cells and/or the amount of signals coming from these cells has to be reached for the *shha*-expressing domain to split. After branching, each sister branch holds one smaller domain of *shha*-expressing cells. As the branches grow, the signals emanating from the *shha*-expressing cells again accumulate until they reach again the threshold necessary for a new splitting. This threshold mechanism may explain the branching delay observed following laser ablation. Indeed, laser ablation eliminates *shha*-expressing cells as well as the signals they release. It may have local effects on the basement membrane separating the *shha*-expressing cells from the scleroblasts. Although the absence of the *shha*-expressing cells is transient due to the regenerative process, when they re-appear, they have to reset the molecular pathways leading to the synthesis of the 'splitting' signal. The time it takes for the accumulation of this signal to reach the splitting threshold level would explain the branching delay.

In conclusion, the transient ablation of shha-expressing cells revealed their importance in controlling branching morphogenesis and argues for a role of these cells in dermal bone patterning.

Acknowledgments

We thank Marc Ekker for critical reading of the manuscript. This work was supported by a Canadian Institute of Health Research (CIHR) grant to M.A.A.

References

Abraham, E., Palevitch, O., Gothilf, Y., Zohar, Y., 2010. Targeted gonadotropin-releasing hormone-3 neuron ablation in zebrafish: effects on neurogenesis, neuronal migration, and reproduction. Endocrinology 151, 332–340.
Affolter, M., Zeller, R., Caussinus, E., 2009. Tissue remodelling through branching morphogenesis. Nat. Rev. Mol. Cell Biol. 10, 831–842.
Akimenko, M.A., Ekker, M., Wegner, J., Lin, W., Westerfield, M., 1994. Combinatorial expression of three zebrafish genes related to distal-less: part of a homeobox gene code for the head. J. Neurosci. 14, 3475–3486.
Akimenko, M.A., Mari-Beffa, M., Becerra, J., Geraudie, J., 2003. Old questions, new tools, and some answers to the mystery of fin regeneration. Dev. Dyn. 226, 190–201.
Andreasen, E.A., Mathew, L.K., Lohr, C.V., Hasson, R., Tanguay, R.L., 2007. Aryl hydrocarbon receptor activation impairs extracellular matrix remodeling during zebra fish fin regeneration. Toxicol. Sci. 95, 215–226.
Avaron, F., Hoffman, L., Guay, D., Akimenko, M.A., 2006. Characterization of two new zebrafish members of the hedgehog family: atypical expression of a zebrafish Indian hedgehog gene in skeletal elements of both endochondral and dermal origins. Dev. Dyn. 235, 478–489.
Bellusci, S., Furuta, Y., Rush, M.G., Henderson, R., Winnier, G., Hogan, B.L., 1997a. Involvement of Sonic hedgehog (Shh) in mouse embryonic lung growth and morphogenesis. Development 124, 53–63.
Bellusci, S., Grindley, J., Emoto, H., Itoh, N., Hogan, B.L., 1997b. Fibroblast growth factor 10 (FGF10) and branching morphogenesis in the embryonic mouse lung. Development 124, 4867–4878.
Boras-Granic, K., Chang, H., Grosschedl, R., Hamel, P.A., 2006. Lef1 is required for the transition of Wnt signaling from mesenchymal to epithelial cells in the mouse embryonic mammary gland. Dev. Biol. 295, 219–231.
Briscoe, J., Chen, Y., Jessell, T.M., Struhl, G., 2001. A hedgehog-insensitive form of patched provides evidence for direct long-range morphogen activity of sonic hedgehog in the neural tube. Mol. Cell 7, 1279–1291.
Chin, H.J., Fisher, M.C., Li, Y., Ferrari, D., Wang, C.K., Lichtler, A.C., Dealy, C.N., Kosher, R.A., 2007. Studies on the role of Dlx5 in regulation of chondrocyte differentiation during endochondral ossification in the developing mouse limb. Dev. Growth Differ. 49, 515–521.
Eastman, Q., Grosschedl, R., 1999. Regulation of LEF-1/TCF transcription factors by Wnt and other signals. Curr. Opin. Cell Biol. 11, 233–240.
Ellies, D.L., Langille, R.M., Martin, C.C., Akimenko, M.A., Ekker, M., 1997. Specific craniofacial cartilage dysmorphogenesis coincides with a loss of dlx gene expression in retinoic acid-treated zebrafish embryos. Mech. Dev. 61, 23–36.
Ertzer, R., Muller, F., Hadzhiev, Y., Rathnam, S., Fischer, N., Rastegar, S., Strahle, U., 2007. Cooperation of sonic hedgehog enhancers in midline expression. Dev. Biol. 301, 578–589.
Ferrari, D., Kosher, R.A., 2002. Dlx5 is a positive regulator of chondrocyte differentiation during endochondral ossification. Dev. Biol. 252, 257–270.
Ferrari, D., Sumoy, L., Gannon, J., Sun, H., Brown, A.M., Upholt, W.B., Kosher, R.A., 1995. The expression pattern of the Distal-less homeobox-containing gene Dlx-5 in the

developing chick limb bud suggests its involvement in apical ectodermal ridge activity, pattern formation, and cartilage differentiation. Mech. Dev. 52, 257–264.
Freestone, S.H., Marker, P., Grace, O.C., Tomlinson, D.C., Cunha, G.R., Harnden, P., Thomson, A.A., 2003. Sonic hedgehog regulates prostatic growth and epithelial differentiation. Dev. Biol. 264, 352–362.
Fu, M., Lui, V.C., Sham, M.H., Pachnis, V., Tam, P.K., 2004. Sonic hedgehog regulates the proliferation, differentiation, and migration of enteric neural crest cells in gut. J. Cell Biol. 166, 673–684.
Fujimori, S., Novak, H., Weissenbock, M., Jussila, M., Goncalves, A., Zeller, R., Galloway, J., Thesleff, I., Hartmann, C., 2010. Wnt/beta-catenin signaling in the dental mesenchyme regulates incisor development by regulating Bmp4. Dev. Biol. 348, 97–106.
Gjorevski, N., Nelson, C.M., 2010. The mechanics of development: models and methods for tissue morphogenesis. Birth Defects Res. C Embryo Today 90, 193–202.
Gordon, C.T., Brinas, I.M., Rodda, F.A., Bendall, A.J., Farlie, P.G., 2010. Role of Dlx genes in craniofacial morphogenesis: Dlx2 influences skeletal patterning by inducing ectomesenchymal aggregation in ovo. Evol. Dev. 12, 459–473.
Gray, R.S., Cheung, K.J., Ewald, A.J., 2010. Cellular mechanisms regulating epithelial morphogenesis and cancer invasion. Curr. Opin. Cell Biol. 22, 640–650.
Greenspoon, S., Patel, C.K., Hashmi, S., Bernhardt, R.R., Kuwada, J.Y., 1995. The notochord and floor plate guide growth cones in the zebrafish spinal cord. J. Neurosci. 15, 5956–5965.
Harris, S.E., Guo, D., Harris, M.A., Krishnaswamy, A., Lichtler, A., 2003. Transcriptional regulation of BMP-2 activated genes in osteoblasts using gene expression microarray analysis: role of Dlx2 and Dlx5 transcription factors. Front. Biosci. 8, s1249–s1265.
Harunaga, J., Hsu, J.C., Yamada, K.M., 2011. Dynamics of Salivary Gland Morphogenesis. J. Dent. Res. 90, 1070–1077.
Hutchin, M.E., Kariapper, M.S., Grachtchouk, M., Wang, A., Wei, L., Cummings, D., Liu, J., Michael, L.E., Glick, A., Dlugosz, A.A., 2005. Sustained Hedgehog signaling is required for basal cell carcinoma proliferation and survival: conditional skin tumorigenesis recapitulates the hair growth cycle. Genes Dev. 19, 214–223.
Jaskoll, T., Leo, T., Witcher, D., Ormestad, M., Astorga, J., Bringas Jr., P., Carlsson, P., Melnick, M., 2004. Sonic hedgehog signaling plays an essential role during embryonic salivary gland epithelial branching morphogenesis. Dev. Dyn. 229, 722–732.
Kim, Y.J., Lee, M.H., Wozney, J.M., Cho, J.Y., Ryoo, H.M., 2004. Bone morphogenetic protein-2-induced alkaline phosphatase expression is stimulated by Dlx5 and repressed by Msx2. J. Biol. Chem. 279, 50773–50780.
Kim, N., Yamamoto, H., Pauling, M.H., Lorizio, W., Vu, T.H., 2009. Ablation of lung epithelial cells deregulates FGF-10 expression and impairs lung branching morphogenesis. Anat. Rec. (Hoboken) 292, 123–130.
Knopf, F., Hammond, C., Chekuru, A., Kurth, T., Hans, S., Weber, C.W., Mahatma, G., Fisher, S., Brand, M., Schulte-Merker, S., Weidinger, G., 2011. Bone regenerates via dedifferentiation of osteoblasts in the zebrafish fin. Dev. Cell 20, 713–724.
Kratochwil, K., Dull, M., Farinas, I., Galceran, J., Grosschedl, R., 1996. Lef1 expression is activated by BMP-4 and regulates inductive tissue interactions in tooth and hair development. Genes Dev. 10, 1382–1394.
Krause, A., Xu, Y., Joh, J., Hubner, R., Gess, A., Ilic, T., Worgall, S., 2010. Overexpression of sonic Hedgehog in the lung mimics the effect of lung injury and compensatory lung growth on pulmonary Sca-1 and CD34 positive cells. Mol. Ther. 18, 404–412.
Laforest, L., Brown, C.W., Poleo, G., Geraudie, J., Tada, M., Ekker, M., Akimenko, M.A., 1998. Involvement of the sonic hedgehog, patched 1 and bmp2 genes in patterning of the zebrafish dermal fin rays. Development 125, 4175–4184.
Lee, M.H., Kim, Y.J., Kim, H.J., Park, H.D., Kang, A.R., Kyung, H.M., Sung, J.H., Wozney, J.M., Ryoo, H.M., 2003a. BMP-2-induced Runx2 expression is mediated by Dlx5, and TGF-beta 1 opposes the BMP-2-induced osteoblast differentiation by suppression of Dlx5 expression. J. Biol. Chem. 278, 34387–34394.
Lee, M.H., Kwon, T.G., Park, H.S., Wozney, J.M., Ryoo, H.M., 2003b. BMP-2-induced Osterix expression is mediated by Dlx5 but is independent of Runx2. Biochem. Biophys. Res. Commun. 309, 689–694.
Lee, Y., Hami, D., De Val, S., Kagermeier-Schenk, B., Wills, A.A., Black, B.L., Weidinger, G., Poss, K.D., 2009. Maintenance of blastemal proliferation by functionally diverse epidermis in regenerating zebrafish fins. Dev. Biol. 331, 270–280.
Levi, G., Mantero, S., Barbieri, O., Cantatore, D., Paleari, L., Beverdam, A., Genova, F., Robert, B., Merlo, G.R., 2006. Msx1 and Dlx5 act independently in development of craniofacial skeleton, but converge on the regulation of Bmp signaling in palate formation. Mech. Dev. 123, 3–16.
Li, Y.X., Zdanowicz, M., Young, L., Kumiski, D., Leatherbury, L., Kirby, M.L., 2003. Cardiac neural crest in zebrafish embryos contributes to myocardial cell lineage and early heart function. Dev. Dyn. 226, 540–550.
Li, Y., Zhang, H., Choi, S.C., Litingtung, Y., Chiang, C., 2004. Sonic hedgehog signaling regulates Gli3 processing, mesenchymal proliferation, and differentiation during mouse lung organogenesis. Dev. Biol. 270, 214–231.
Miller, L.A., Wert, S.E., Clark, J.C., Xu, Y., Perl, A.K., Whitsett, J.A., 2004. Role of Sonic hedgehog in patterning of tracheal–bronchial cartilage and the peripheral lung. Dev. Dyn. 231, 57–71.
Moore, K.A., Polte, T., Huang, S., Shi, B., Alsberg, E., Sunday, M.E., Ingber, D.E., 2005. Control of basement membrane remodeling and epithelial branching morphogenesis in embryonic lung by Rho and cytoskeletal tension. Dev. Dyn. 232, 268–281.
Mullor, J.L., Guerrero, I., 2000. A gain-of-function mutant of patched dissects different responses to the hedgehog gradient. Dev. Biol. 228, 211–224.
Park, J., Zhang, J.J., Moro, A., Kushida, M., Wegner, M., Kim, P.C., 2010. Regulation of Sox9 by Sonic Hedgehog (Shh) is essential for patterning and formation of tracheal cartilage. Dev. Dyn. 239, 514–526.
Patel, V.N., Rebustini, I.T., Hoffman, M.P., 2006. Salivary gland branching morphogenesis. Differentiation 74, 349–364.
Pepicelli, C.V., Lewis, P.M., McMahon, A.P., 1998. Sonic hedgehog regulates branching morphogenesis in the mammalian lung. Curr. Biol. 8, 1083–1086.
Poleo, G., Brown, C.W., Laforest, L., Akimenko, M.A., 2001. Cell proliferation and movement during early fin regeneration in zebrafish. Dev. Dyn. 221, 380–390.
Poss, K.D., Shen, J., Keating, M.T., 2000. Induction of lef1 during zebrafish fin regeneration. Dev. Dyn. 219, 282–286.
Poss, K.D., Keating, M.T., Nechiporuk, A., 2003. Tales of regeneration in zebrafish. Dev. Dyn. 226, 202–210.
Pu, Y., Huang, L., Prins, G.S., 2004. Sonic hedgehog-patched Gli signaling in the developing rat prostate gland: lobe-specific suppression by neonatal estrogens reduces ductal growth and branching. Dev. Biol. 273, 257–275.
Quint, E., Smith, A., Avaron, F., Laforest, L., Miles, J., Gaffield, W., Akimenko, M.A., 2002. Bone patterning is altered in the regenerating zebrafish caudal fin after ectopic expression of sonic hedgehog and bmp2b or exposure to cyclopamine. Proc. Natl. Acad. Sci. U. S. A. 99, 8713–8718.
Roeser, T., Baier, H., 2003. Visuomotor behaviors in larval zebrafish after GFP-guided laser ablation of the optic tectum. J. Neurosci. 23, 3726–3734.
Sekine, K., Ohuchi, H., Fujiwara, M., Yamasaki, M., Yoshizawa, T., Sato, T., Yagishita, N., Matsui, D., Koga, Y., Itoh, N., Kato, S., 1999. Fgf10 is essential for limb and lung formation. Nat. Genet. 21, 138–141.
Smith, A., Avaron, F., Guay, D., Padhi, B.K., Akimenko, M.A., 2006. Inhibition of BMP signaling during zebrafish fin regeneration disrupts fin growth and scleroblasts differentiation and function. Dev. Biol. 299, 438–454.
Smith, A., Zhang, J., Guay, D., Quint, E., Johnson, A., Akimenko, M.A., 2008. Gene expression analysis on sections of zebrafish regenerating fins reveals limitations in the whole-mount in situ hybridization method. Dev. Dyn. 237, 417–425.
Thomson, A.A., Marker, P.C., 2006. Branching morphogenesis in the prostate gland and seminal vesicles. Differentiation 74, 382–392.
Towers, M., Mahood, R., Yin, Y., Tickle, C., 2008. Integration of growth and specification in chick wing digit-patterning. Nature 452, 882–886.
Tu, S., Johnson, S.L., 2011. Fate restriction in the growing and regenerating zebrafish fin. Dev. Cell 20, 725–732.
van Genderen, C., Okamura, R.M., Farinas, I., Quo, R.G., Parslow, T.G., Bruhn, L., Grosschedl, R., 1994. Development of several organs that require inductive epithelial–mesenchymal interactions is impaired in LEF-1-deficient mice. Genes Dev. 8, 2691–2703.
Vieux-Rochas, M., Mantero, S., Heude, E., Barbieri, O., Astigiano, S., Couly, G., Kurihara, H., Levi, G., Merlo, G.R., 2010. Spatio-temporal dynamics of gene expression of the Edn1–Dlx5/6 pathway during development of the lower jaw. Genesis 48, 262–373.
Vihtelic, T.S., Hyde, D.R., 2000. Light-induced rod and cone cell death and regeneration in the adult albino zebrafish (*Danio rerio*) retina. J. Neurobiol. 44, 289–307.
Westerfield, M., 1993. The Zebrafish Book. Eugene: University of Oregon Press.
Widelitz, R.B., Jiang, T.X., Lu, J., Chuong, C.M., 2000. beta-catenin in epithelial morphogenesis: conversion of part of avian foot scales into feather buds with a mutated beta-catenin. Dev. Biol. 219, 98–114.
Wu, D., Freund, J.B., Fraser, S.E., Vermot, J., 2011. Mechanistic basis of otolith formation during teleost inner ear development. Dev. Cell 20, 271–278.
Yuasa, T., Kataoka, H., Kinto, N., Iwamoto, M., Enomoto-Iwamoto, M., Iemura, S., Ueno, N., Shibata, Y., Kurosawa, H., Yamaguchi, A., 2002. Sonic hedgehog is involved in osteoblast differentiation by cooperating with BMP-2. J. Cell. Physiol. 193, 225–232.
Zhao, G.Q., Zhao, S., Zhou, X., Eberspaecher, H., Solursh, M., de Crombrugghe, B., 1994. rDlx, a novel distal-less-like homeoprotein is expressed in developing cartilages and discrete neuronal tissues. Dev. Biol. 164, 37–51.
Zhu, H., Bendall, A.J., 2009. Dlx5 is a cell autonomous regulator of chondrocyte hypertrophy in mice and functionally substitutes for Dlx6 during endochondral ossification. PLoS One 4, e8097.